CWE-8
June 7-11, 2026
London, ON, Canada

Numerical Validation of a Naturally Ventilated Double-Skin BIPV Façade and Configuration Impact on Cell Temperatures

Fatma Abdul Hameed, Anwar Awol, Muna Younis, Girma T. Bitsuamlak

Department of Civil and Environmental Engineering/Boundary Layer Wind Tunnel Laboratory/WindEEE Research Institute, Western University, ON, Canada.

SUMMARY

Building-integrated photovoltaics (BIPV) function as façade elements with effective albedo values that vary according to cell temperature-dependent operational efficiency. This study employs computational fluid dynamics (CFD) to capture multi-energy interactions at the BIPV façade scale, including spatial thermal variations, wind direction, surrounding context, building geometry, radiative effects, and both natural and forced convection. Model outputs achieved 1–3% accuracy in predicting back-of-module temperatures (BOMT) under semi-windward, naturally ventilated conditions when validated against an experimental study from the literature. Additional cases were developed to investigate ventilation effectiveness under varying wind directions and segmented versus continuous façade configurations. Results indicate that variations in convective heat transfer coefficients (CHTC) across these configurations can lead to operating temperature changes of up to 4.5°C. By resolving the spatial variability of CHTC at the façade scale, this work supports more reliable early-stage assessment of BIPV performance and informs design decisions related to façade configuration, ventilation strategy, and wind exposure.

Keywords: *BIPV, cell temperature, CFD, spatial thermal variations, naturally ventilated, CHTC*

1. INTRODUCTION

Solar energy is considered an ideal renewable source due to its sustainability and availability. Nearly zero-energy buildings (NZEB) leverage environmental benefits such as strategic building placement, orientation, and active façades. BIPV systems have the potential to provide the built environment with next-generation sustainable façades that generate both electricity and heat. Design-informed configurations and placements of BIPV systems can significantly influence energy output. Common configurations include close-mount, curtain wall, or double-skin wall (Martín-Chivelet et al., 2022). Double-skin walls enable natural ventilation of solar modules through a mounting frame, allowing improved electrical efficiency as heat is dissipated and operating temperature is reduced per:

$$\eta_{c,operation} = \eta_{c,STC}\, x \left[1 - \frac{\beta}{100}(T_{op} - 25)\right] \quad (1)$$

where $\eta_{c,operation}$ is the efficiency during operation, $\eta_{c,STC}$ is the electrical efficiency under STC, T_{op} is the operating temperature of the solar cells (ºC), and β is the change in efficiency per temperature deviation from 25 °C (%/°C).

Although previous studies have examined the thermal performance of BIPV systems, many approaches simplified airflow interactions, relied on multiple solvers, or neglected radiative effects due to study scope. As a result, there remains a need for a unified modelling approach that simultaneously accounts for spatial thermal variations, wind direction, surrounding context, building geometry, radiative effects, and both natural and forced convection. To address this gap, this study develops a CFD-based modelling framework for BIPV façades that integrates these coupled physics processes. The model is evaluated using manufacturer specifications and a full-scale experimental structure. An empirical model developed by Sandia National Laboratories (SNL) (Kratochvil et al., 2004) is used to classify the rear ventilation effectiveness of the experimental configuration, providing context. The validated framework is then applied to investigate the influence of wind direction and segmented versus continuous façade configurations on BIPV thermal performance.

2. METHODS

An experimental structure in Dubai, UAE (Alhammadi et al., 2022), includes west, east, and south naturally ventilated BIPV façades with c-Si and CIGS solar cell materials (Figure 1). The ventilation gap is open to the surrounding environment at ground level and roof opening, with a gap width of 8.3 cm. Each façade includes vertical and horizontal segmentations of 1.2 cm. Temperature sensors (period: 30 seconds) were placed at the center and back of each solar module, providing statistical averages, maxima, and minima over selected time periods. Two of these periods were replicated in the CFD simulation using corresponding inputs: weather data, material specifications, and generalized assumptions. For these periods, the average BOMT of the south façade served as the validation parameter. The south façade experienced northwest wind in the first case and southwest wind in the second case. The CFD model includes a control volume for the environmental surroundings with temperature-dependent air properties and a building-level control volume with solar modules characterized by a volumetric heat source boundary condition (Figure 2). The air control volume incorporates the following physics models: steady-state Reynolds-Averaged Navier-Stokes (RANS), segregated energy, Boussinesq approximation, gravity, gray thermal radiation, and surface-to-surface radiation. The inflow velocity is characterized by the atmospheric boundary layer (ABL) and SST (shear stress transport) k-ω turbulence model, as recommended by literature (Defraeye et al., 2010; Kahsay et al., 2019; Karava et al., 2011; Younis et al., 2023), to achieve high-resolution surface parameters. Additional study cases were derived from the experimental structure by focusing on a single façade and evaluating performance under different wind directions and segmentation configurations.

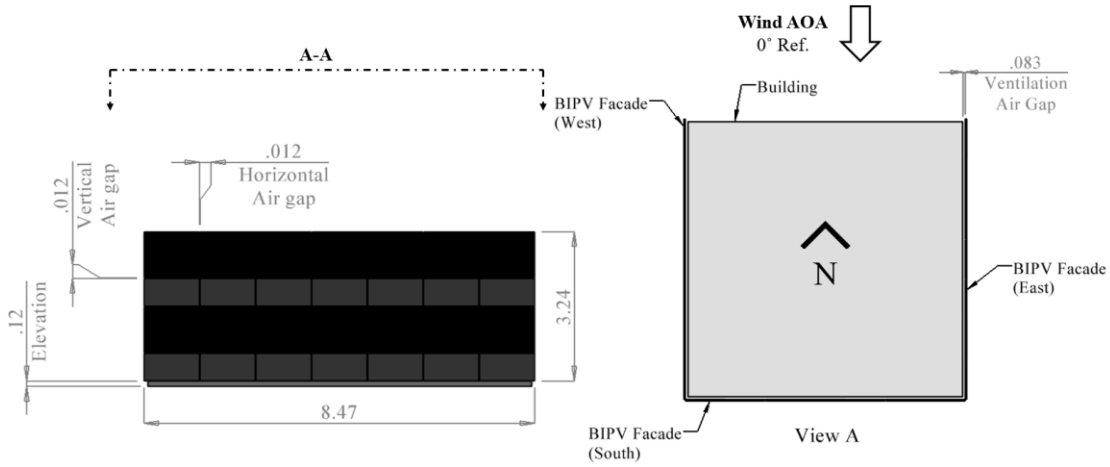

Figure 1: BIPV Experimental Structure (Represented based on information provided by (Alhammadi et al., 2022))

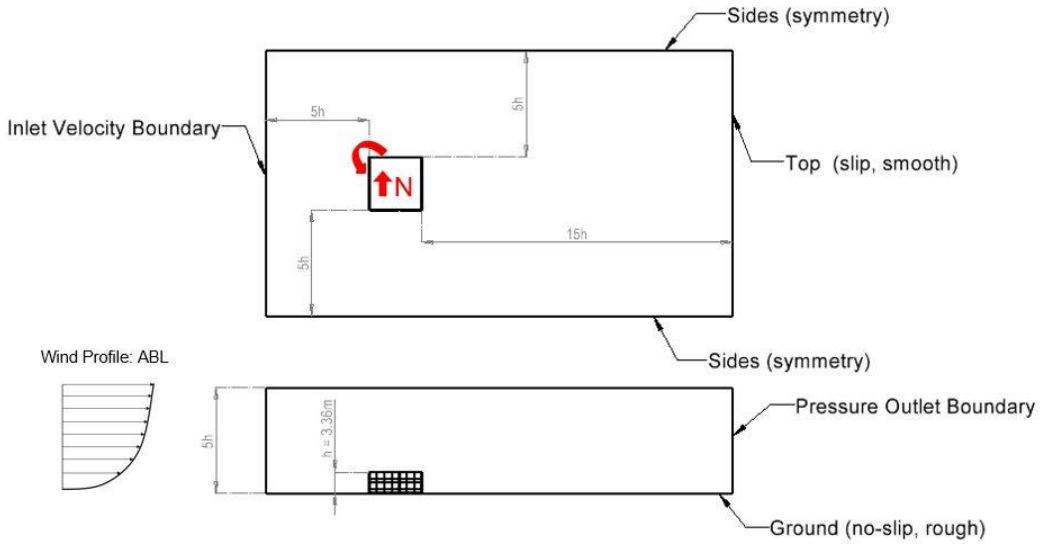

Figure 2: Experimental Structure CFD Model

The airflow domain is discretized with polyhedral mesh cells and includes two control volumes that gradually reduce the base mesh size of 1 m. The building and solar module surfaces (no-slip boundary condition) are further refined and include 12 prism layers; the first cell height is 0.26 mm, corresponding to the viscous sublayer. Mesh independence was evaluated (±10%) based on resulting wall y^+ values. The finer mesh configuration, consisting of approximately 37 million cells, was selected as it achieved a wall y^+ value of 1 on the solar module surfaces (Blocken et al., 2009).

3. RESULTS AND DISCUSSIONS

3.1. Validation

Based on the two cases used for the average BOMT comparison of the south façade, higher accuracy was achieved in the second case. In the first case, the south façade is exposed to the recirculation zone of the wind flow, where surface parameters such as temperature are strongly sensitive (Figure 3). As a result, the average BOMT was underestimated by 11–15%. In contrast, in the second case, turbulence has a reduced influence on surface parameters because the façade is in a semi-windward orientation, leading to a BOMT underestimation of only 1–3%. Due to differences in ambient conditions, the effectiveness of natural ventilation in Cases 1 and 2 is classified as "medium" and "good" rear ventilation, respectively, according to the SNL empirical model. This highlights the limitations of empirical models for applications that are highly sensitive to ambient conditions, as such variations can significantly alter the convective heat transfer coefficient (CHTC).

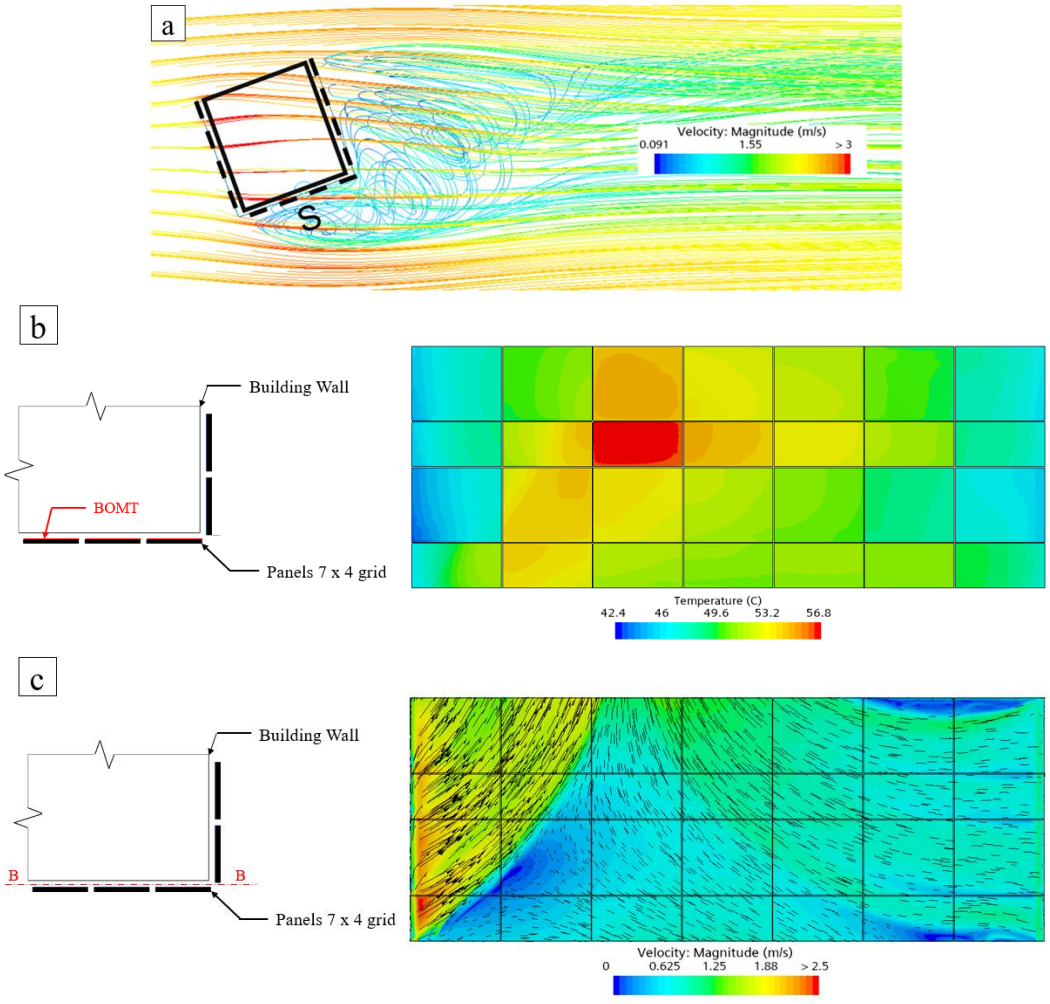

Figure 3: Case 1 - a) Top view velocity streamlines b) BOMT contour plot and c) Mid-gap thickness section B-B velocity plot

3.2. Study Cases

In the study case analysis, wind direction was found to have a significantly greater impact on the CHTC (Table 1) than the introduction of vertical or horizontal segmentations (1.2 cm). Sideward and windward directions reduced operating temperatures by an average of 2.40°C and 4.50°C, respectively, compared to the leeward direction. The total variance in operating cell temperatures, ΔT_{op}, is a key indicator of a common BIPV failure mode known as hotspot occurrence. Within the scope of this study, the variance in operating cell temperatures remained modest relative to the critical threshold of 20°C (Moretón et al., 2015). The sideward configuration exhibited the highest ΔT_{op} (6.3-6.5°C), attributed to mixed-mode interactions involving wind separation and reattachment along the façade, which resulted in spatial variability in heat exchange. In the windward case, and for the continuous façade configuration, heat accumulation with height was prominent, resulting in higher operating temperatures for solar cells at elevated positions. In contrast, the segmented façade configuration allowed wind flow to enter along the height of the façade, offsetting this effect. This behavior is quantified by an overall improvement of 2.12 W/m^{2}K in CHTC, an enhancement not observed for the other wind directions. These findings indicate that the benefits of façade segmentation may be outweighed by the stronger influence of wind attack angle. For large-scale façade implementations, even relatively small changes in operational efficiency can have a meaningful impact on annual energy production, and ΔT_{op} may approach critical thresholds.

Table 1: Study case results of windward & leeward segmented configurations

Configuration	Solar Cell	Mean T_{op} (°C)	ΔT_{op} (°C)	$\eta_{c,operation}$ (%)	CHTC (W/m^{2}K)
Windward	c-Si	54.16	2.10	13.49	13.54
	CIGS	54.71	2.07	11.16	13.54
Leeward	c-Si	58.71	4.54	13.18	5.98
	CIGS	59.24	5.85	10.96	5.98

ΔT_{op} – Total variance in operating cell temperatures within each configuration

4. CONCLUSION

This study presents a definite CFD-based framework for evaluating the thermal performance of naturally ventilated BIPV double-skin façades under realistic wind and environmental conditions. Validation against full-scale experimental data demonstrated strong agreement under semi-windward conditions, with BOMT prediction errors within 1–3%, highlighting the capability of the model to capture coupled convective, radiative, and buoyancy-driven heat transfer processes at the solar module scale. Parametric analyses revealed that wind direction is the dominant factor influencing convective heat transfer and operating temperatures, exceeding the impact of façade segmentation for the configurations studied. While segmentation can locally enhance ventilation under specific wind exposures, its effectiveness is highly dependent on wind attack angle and was diminished under leeward or sideward conditions. The spatial variability of CHTC and operating temperatures further emphasizes the limitations of empirical models for BIPV systems exposed to urban wind environments. By resolving façade-scale airflow and heat transfer mechanisms, the proposed modelling framework enables more reliable early-stage design assessment of BIPV systems, supporting informed decisions regarding façade configuration, orientation, and ventilation strategy. The findings underscore the importance of accounting for wind exposure in large-scale BIPV implementations, where even small reductions in operating temperature and temperature variance can yield meaningful improvements in long-term energy performance and system reliability. The observed moderate discrepancies, particularly in cases sensitive to the approximation of the recirculation zone, can be attributed to the steady-state assumption adopted in this study. These discrepancies could be reduced by employing time-resolved simulations using URANS or LES approaches.

5. REFERENCES

Alhammadi, N., Rodriguez-Ubinas, E., Alzarouni, S., Alantali, M., 2022. Building-integrated photovoltaics in hot climates: Experimental study of CIGS and c-Si modules in BIPV ventilated facades. Energy Convers. Manag. 274, 116408. https://doi.org/10.1016/j.enconman.2022.116408

Blocken, B., Defraeye, T., Derome, D., Carmeliet, J., 2009. High-resolution CFD simulations for forced convective heat transfer coefficients at the facade of a low-rise building. Build. Environ. 44, 2396–2412. https://doi.org/10.1016/j.buildenv.2009.04.004

Defraeye, T., Blocken, B., Carmeliet, J., 2010. CFD analysis of convective heat transfer at the surfaces of a cube immersed in a turbulent boundary layer. Int. J. Heat Mass Transf. 53, 297–308. https://doi.org/10.1016/j.ijheatmasstransfer.2009.09.029

Goncalves, J.E., Van Hooff, T., Saelens, D., 2020. Understanding the behaviour of naturally-ventilated BIPV modules: A sensitivity analysis. Renew. Energy 161, 133–148. https://doi.org/10.1016/j.renene.2020.06.086

Kahsay, M.T., Bitsuamlak, G., Tariku, F., 2019. Numerical analysis of convective heat transfer coefficient for building facades. J. Build. Phys. 42, 727–749. https://doi.org/10.1177/1744259118791207

Karava, P., Jubayer, C.M., Savory, E., 2011. Numerical modelling of forced convective heat transfer from the inclined windward roof of an isolated low-rise building with application to photovoltaic/thermal systems. Appl. Therm. Eng. 31, 1950–1963. https://doi.org/10.1016/j.applthermaleng.2011.02.042

Kratochvil, J., Boyson, W., King, D., 2004. Photovoltaic array performance model. (No. SAND2004-3535, 919131). Sandia National Laboratories. https://doi.org/10.2172/919131

Martín-Chivelet, N., Kapsis, K., Wilson, H.R., Delisle, V., Yang, R., Olivieri, L., Polo, J., Eisenlohr, J., Roy, B., Maturi, L., Otnes, G., Dallapiccola, M., Upalakshi Wijeratne, W.M.P., 2022. Building-Integrated Photovoltaic (BIPV) products and systems: A review of energy-related behavior. Energy Build. 262, 111998. https://doi.org/10.1016/j.enbuild.2022.111998

Moretón, R., Lorenzo, E., Narvarte, L., 2015. Experimental observations on hot-spots and derived acceptance/rejection criteria. Sol. Energy 118, 28–40. https://doi.org/10.1016/j.solener.2015.05.009

Younis, M., Kahsay, M.T., Bitsuamlak, G.T., 2023. BIM-CFD-based Thermal Analysis for Northern Buildings on Permafrost. J. Cold Reg. Eng. 37, 04023019. https://doi.org/10.1061/JCRGEI.CRENG-644